CIMAC CONGRESS 25
ZURICH, MAY 19 – 23, 2025

2025 | 349

Research on Unbalanced Fault Diagnosis of Marine Turbocharger Rotor Based on Transfer Learning

Turbochargers & Air/Exhaust Management

Luyuan Liu, School of Naval Architecture, Ocean and Energy Power Engineering, Wuhan University of Technology, Wuhan 430063, China

Lei Hu, School of Naval Architecture, Ocean and Energy Power Engineering, Wuhan University of Technology, Wuhan 430063, China
Fei Dong, School of Naval Architecture, Ocean and Energy Power Engineering, Wuhan University of Technology, Wuhan 430063, China
Jiahong Zhong, Chongqing Jiangjin Shipbuilding Industry Co Lgtd, Chongqing 402289, China
Jianguo Yang, School of Naval Architecture, Ocean and Energy Power Engineering, Wuhan University of Technology, Wuhan 430063, China
Can Zheng, China Energy Engineering Group Guangdong Electric Power Design Institute Co.,Ltd., Guangzhou 510663, China

DOI: https://doi.org/10.5281/zenodo.15222970

ABSTRACT

The simulation test for rotor imbalance faults in turbochargers has high costs and may bring destructive risks to the entire machine. At the same time, the variable speed working characteristics of turbochargers bring great difficulties in fault diagnosis. Regarding the above issues, a certain marine turbocharger is taken as an object in the paper, and finite element models are established in both fluid and solid domains. By setting the boundary conditions from the experimentation and design of the turbocharger, the fluid excitation forces at the turbine and compressor are calculated using Fluent software. The comprehensive vibration response model of the turbocharger is established using the modal reduction and rotor dynamics analysis based on Workbench software. Experimental vibration data from the base of the turbocharger under normal operating conditions are collected and compared with simulation results to validate the model. Dynamic unbalanced faults of the rotor are simulated using a model reconstruction approach at various speeds, and the patterns of vibration responses at different fault severities are analyzed. Characteristic parameter datasets for rotor unbalanced vibration in both the source and target domains are simulated and extracted. The convolutional neural network (CNN) model is established based on the vibration data from the base of the turbocharger and pre-trained using data from the source domain. The Maximum Mean Difference (MMD) is measured for the feature distribution distance between the source and target domains at each layer of the pre-trained model. The effectiveness of convolutional layer and fully connected layer migration is determined by MMD. The model is trained again using the labeled target domain data to classify and identify fault data in the target domain. The study demonstrates that the error of the established turbocharger vibration response simulation model is within 5%, the method based on the CNN transfer learning model can effectively diagnose the degree of rotor imbalance under variable speed operating conditions of the turbocharger and has a high diagnostic accuracy.

1 INTRODUCTION

As one of the indispensable core components of marine power systems, the turbocharger utilizes the energy from the exhaust gases expelled by the engine to drive the turbine, which in turn drives the compressor impeller coaxial with the turbine to rotate at high speed, thus improving the engine's efficiency. At the same time, the compressor compresses air into the engine cylinders, increasing the amount of air, which allows for more efficient fuel utilization and enhances the engine's power.

A recent survey by the Swedish Club on claims related to marine engine damage highlighted that turbocharger failures account for a significant proportion, representing 27.34% of all engine failures [1]. The rotor, essential to the turbocharger, is pivotal in ensuring operational stability. Imbalances in the rotor can originate from several factors: disparities in material quality, errors during manufacturing and installation, as well as operational challenges such as thermal deformation, wear, and media adhesion. Collectively, these elements lead to the inertia shaft of rotor inevitably deviating from the rotational axis [2]. The phenomenon of rotor unbalanced can affect the stability and lifespan of the turbocharger itself, leading to unstable compressed air flow and pressure, thereby reducing the power output and fuel efficiency of the marine engines. Therefore, timely diagnosis of rotor imbalance fault is of great significance to ensure the dynamic performance of the turbocharger and enhance the performance and reliability of the marine engine.

Both at home and abroad, the phenomenon of rotor imbalance is studied extensively. Ahobal et al. conduct a harmonic analysis of the rotor imbalance vibration signals, revealing that the rotor system exhibits different response characteristics in response to various unbalanced masses [3]. Knotek et al. investigate the impact of imbalance magnitude on the dynamic behavior of the turbocharger rotor through simulation [4]. Bin et al. construct a finite element solid model of the turbocharger rotor-bearing system, which is used to determine the optimal configuration scheme for the imbalance excitation on the rotor [5]. In summary, research on the influence law of turbocharger rotor imbalance is relatively mature both domestically and internationally. However, there is a lack of research concerning the diagnosis of rotor unbalanced faults.

Accordingly, this paper establishes a vibration response model for the complete marine turbocharger system, based on the analysis of a certain marine turbocharger. This model is employed to simulate the rotor imbalance fault, aiding in the analysis of the variations in the turbocharger's vibration response under different speeds and fault severities. Furthermore, a one-dimensional convolutional neural networks (CNN) transfer learning algorithm is devised to diagnose fault vibrations in the rotor imbalance of the turbocharger.

2 THE ESTABLISHMENT OF THE VIBRATION RESPONSE MODEL FOR MARINE TURBOCHARGER SYSTEM

2.1 Division of finite element mesh

The turbocharger is mainly divided into the shell and rotor. To satisfy the simulation requirements for the vibration response of the turbocharger, the three-dimensional solid domain models of the shell and rotor are geometrically cleaned by Hypermesh. The removal of technological features, such as bosses, oil holes, fillets, and chamfers, is conducted as part of the geometric cleaning process, which has minimal impact on the overall vibration of the turbocharger. Subsequently, the fluid domain is extracted from the solid domain on the basis of the turbocharger's operating principles. The final finite element model is shown in Figure 1, in which a first-order tetrahedral mesh is employed to discretize the geometric models of both the solid and fluid domains. The solid domain comprises approximately 489,500 elements, while the fluid domain contains around 25,824,400 elements. The mesh types employed are Solid185 for the solid domain and Shell181 for the fluid domain.

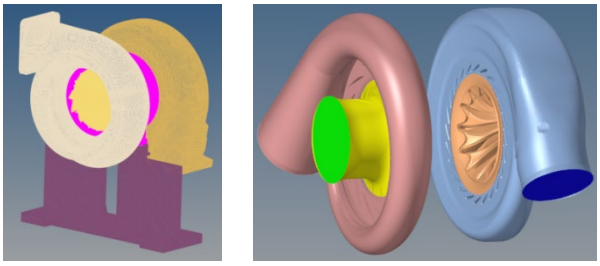

(a) Solid element model (b) Fluid element model

Figure 1. Finite element model of the turbocharger

2.2 Calculation of fluid excitation

A flow field analysis model of the turbocharger is constructed using Ansys Fluent with the objective of calculating the transient fluid excitation on the casing, as shown in Figure 2. The transient solution is set with 1,800 time steps, where each time step corresponds to a 1° rotation of the rotor. In order to guarantee convergence at each step, the maximum number of iterations per step is set to 20. The convergence criterion for the calculation is that the root mean square (RMS) residual must be less than 10^{-4}. Once the transient solution is completed and the results are confirmed to have converged, the

excitation in each direction is output. Figure 3 depicts the variation of the turbocharger fluid excitation over a cycle concerning the iteration steps when the rotor speed is 60,000 rpm.

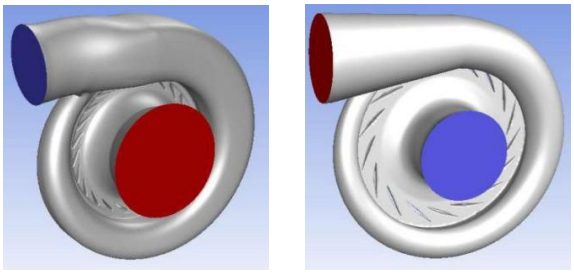

(a)Turbine (b)Compressor

Figure 2. Turbocharger flow field fluid mechanics model

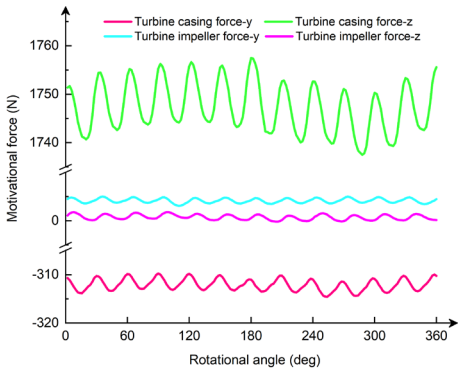

(a)Turbine

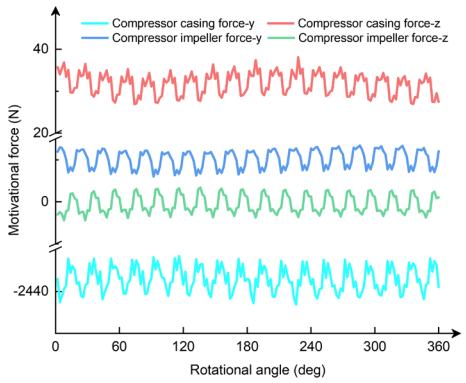

(b)Compressor

Figure 3. Time-domain excitation of the turbocharger fluid domain

2.3 Transient vibration response analysis and model validation

A transient dynamic model of the entire turbocharger is constructed using the Transient Structural module in Ansys Workbench. The connections, constraints, and load boundary conditions between the components of the turbocharger are defined in accordance with established engineering practice. A fixed time step method is employed to define the simulation parameters, and vibration response calculations and analysis of the turbocharger are conducted to obtain the vibration responses of the turbocharger components and the machine feet, as shown in Figure 4.

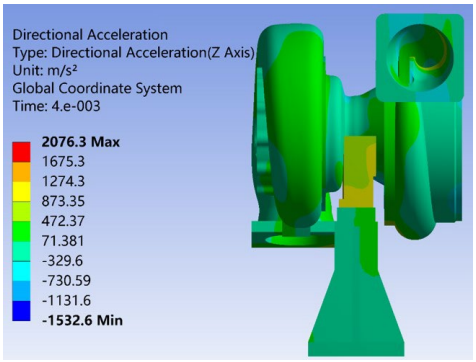

Figure 4. Vibration acceleration contour map of the turbocharger

In order to guarantee the precision of the simulation model for the vibration response of the marine turbocharger assembly, vibration tests of the turbocharger machine feet under standard operational conditions are carried out on the turbocharger performance test bench. The veracity of the model is substantiated through a comparative analysis of the simulation data with the experimental data under standard operational conditions. In view of the challenging working environment of the turbocharger, which is characterised by elevated noise levels, a robust data extraction methodology is employed with a view to extracting meaningful insights from the experimental data, minimising the impact of noise interference and enhancing the precision of the analysis. This is accomplished through the elimination of outlier data in accordance with the three-sigma criterion. Furthermore, a low-pass filter is utilised to remove frequencies that fall outside the sensor's measurement range from the signal.

The experimental and simulation data pertaining to the vibration acceleration signal of the engine mount under normal operating conditions are extracted and subjected to comparison, as shown in Figure 5 and Table 1.

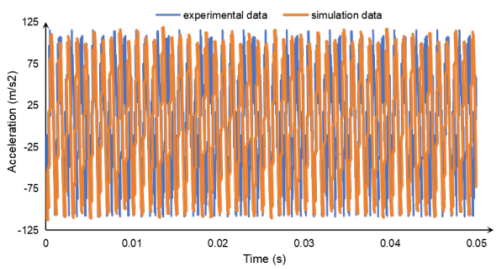

(a)Engine mount vibration acceleration time domain signal comparison

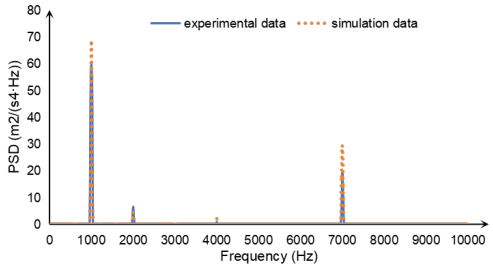

(b)Engine mount power spectral density comparison

Figure 3. Comparison of turbocharger vibration response signals under normal operating conditions at 60,000 rpm

Table 1. Comparison of turbocharger vibration response signal characteristics under normal operating conditions at varying speeds

Speed (r/min)	Feature type	Measured data	Simulated data	Error (%)
	RMS/(m/s^2)	3.73	3.72	0.27
35000	Peak[1]/(m/s^2)	16.55	15.92	3.81
	Frequency[2]/Hz	992	1000	0.81
	RMS/(m/s^2)	6.12	5.87	4.09
40000	Peak[1]/(m/s^2)	28.28	28.53	0.88
	Frequency[2]/Hz	1014	1000	1.38
	RMS/(m/s^2)	7.56	7.46	1.32
45000	Peak[1]/(m/s^2)	31.98	32.52	1.69
	Frequency[2]/Hz	1017	1000	1.67
	RMS/(m/s^2)	12.47	12.03	3.53
50000	Peak[1]/(m/s^2)	52.73	51.55	2.24
	Frequency[2]/Hz	986	1000	1.42
	RMS/(m/s^2)	19.61	19.72	0.56
55000	Peak[1]/(m/s^2)	63.57	63.34	0.36
	Frequency[2]/Hz	979	1000	2.15
	RMS/(m/s^2)	29.01	28.69	1.10
60000	Peak[1]/(m/s^2)	92.98	96.96	4.28
	Frequency[2]/Hz	1035	1000	2.38

[1]Peak-to-peak
[2]PSD max peak frequency

It can be observed that, in the time domain the signal of the base vibration, along with the calculated vibration characteristics such as RMS and peak-to-peak values, are generally consistent with the measured results, with a maximum error of 4.28%. In the frequency domain, the measured and simulated PSD demonstrate a high degree of correlation between the fundamental frequency and its associated harmonic peak frequencies. The maximum peak is observed to occur near the fundamental frequency in both cases. In conclusion, the accuracy of the turbocharger vibration response model is relatively high, which can provide valuable guidance for fault diagnosis research.

3 ROTOR UNBALANCE FAULT SIMULATION ANALYSIS

3.1 Fault simulation modelling method

Due to the high rotational speed of the turbocharger rotor, the asymmetric mass distribution generates centrifugal forces when the rotor rotates at high speeds, causing significant vibrations in the turbocharger. To better simulate the actual rotor unbalance fault condition, an unbalance force is introduced and the calculation formula is as follows:

$$F = me\omega^2 \tag{1}$$

The unbalanced force in the rotor system, not including the shaft, is projected in two directions (in this case the Y-axis and the Z-axis direction) as follows:

$$\begin{cases} F_y = me\omega^2\cos(\omega t) \\ F_z = me\omega^2\sin(\omega t) \end{cases} \tag{2}$$

In Eq.1 and Eq.2, F is the unbalanced force in N; m is the unbalanced mass in g; e is the eccentricity between the unbalanced mass and the center of rotation in mm; ω is the rotational speed of the rotor system in rad/s; t represents a specific time during the rotation of the rotor system in s.

From Eq.2, it can be seen that the effect of unbalance is equivalent to the application of two mutually perpendicular harmonic forces along the Y and Z directions of the rotor axis. Therefore, to simulate the rotor unbalance fault, the unbalance forces F_y and F_z in the two perpendicular directions are applied to the equivalent axis of the rotor system at the node with no weight, thereby achieving the simulation of rotor unbalance errors.

3.2 Rotor imbalance fault simulation analysis

In the actual manufacture and operation of rotor systems, various factors always result in the rotor not reaching a perfectly ideal state, so there will always be some degree of imbalance. Through actual measurements, it is found that the rotor imbalance of this turbocharger under normal operating conditions is 3g·mm.

In order to better describe the extent of rotor imbalance faults, experience is shown that rotor imbalance faults are divided into three categories: normal operating conditions, minor faults, and major faults. It is assumed that the rotor imbalance is 9 g-mm under minor fault conditions and 15 g-mm under severe fault conditions. Using the method of applying the rotor imbalance force described above, a study is made of the variation

of the vibration response at the compressor foot under different rotor speeds and fault severity levels. The results of the simulation analysis are shown in Figure 6-7.

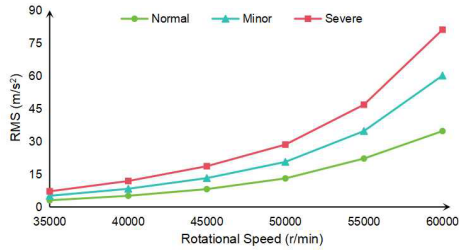

(a)RMS value variation pattern

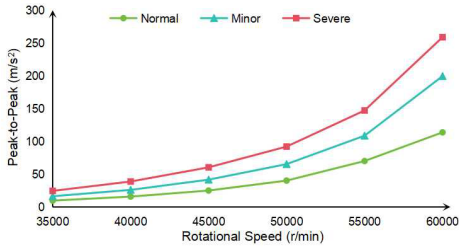

(b)Peak-to-Peak value variation pattern

Figure 6. Variation of vibration characteristics at the compressor foot under different states and rotational speeds

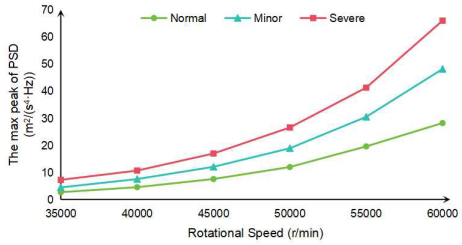

Figure 7. Variation of the maximum peak of PSD at the compressor foot under different states and rotational speeds

Figure 6 shows that as the speed increases and the fault severity increases, both the peak-to-peak value and the RMS value of the vibration acceleration at the base of the turbocharger also increase, with the rate of increase becoming more pronounced. In addition, the power spectral density analysis of the base of turbocharger vibration at different speeds and fault severities shows that rotor imbalance faults generate distinct peaks in the frequency spectrum, with the maximum peak always corresponding to the fundamental frequency. This is because the periodic vibration induced by the unbalanced force is directly related to the speed of rotation, resulting in a concentration of energy at the corresponding frequency. Other harmonic components, such as the second harmonic, fifth harmonic, etc., may also appear, but their amplitudes are generally smaller than those of the fundamental frequency. As shown in Figure 7, it can be observed that as the speed and severity of the fault increase, the maximum peak corresponding to the fundamental frequency in the power spectral density also increases accordingly.

4 DIAGNOSIS OF COMPRESSOR ROTOR IMBALANCE FAULT BASED ON 1D-CNN TRANSFER LEARNING

4.1 Construction of 1D-CNN model and transfer learning

CNN, as a typical deep learning architecture, has powerful capabilities in data mining and information fusion, and is therefore very promising in the fields of feature extraction and multi-source information fusion, and has significant application and research potential [6-9].

The 1D-CNN is mainly used for data classification. Its basic structure consists of the following layers: input layer, convolutional layer, activation function, pooling layer, fully connected layer, and output layer. The structure of the 1D-CNN model constructed in this paper is shown in Figure 8. The activation function of the convolutional layers is ReLU and the activation function of the output layer is Softmax. The convolutional kernels used are large, which helps to extract short-term features, provide more information to the deeper layers of the network, and better suppress high-frequency noise. During backpropagation, the Adam optimization algorithm is used to adaptively adjust the learning rate to optimize the parameters of the network model, thereby obtaining the optimal parameter values and ensuring that the loss function L is minimized.

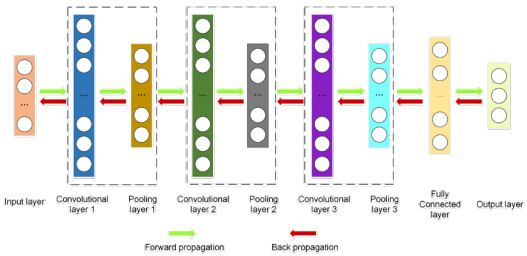

Figure 8. Structure of the 1D-CNN model

The fault diagnosis method based on CNN models has already achieved good diagnostic results in the field of rotating machinery fault diagnosis. However, its implementation requires meeting two conditions: 1) a sufficiently large amount of sample data; and 2) data that is independent and identically distributed. In practical applications, due to the high cost, significant risks, and the difficulty of diagnosing variable speed conditions in rotor imbalance fault simulation tests for marine turbochargers, the actual rotor imbalance vibration

data obtained is often difficult to meet the two conditions mentioned above. This directly affects the accuracy of fault diagnosis. To overcome the limitations of the CNN-based fault diagnosis method, this paper introduces a transfer learning strategy and proposes a new fault diagnosis method, as shown in Figure 9. Transfer learning breaks the assumption that the training and test data in CNN-based fault diagnosis come from the same distribution, while also addressing the problem of insufficient training samples [10-12].

During the transfer process, Maximum Mean Discrepancy (MMD) is used to measure the distance between the feature distributions of the source and target domains. Assume there are two sets of data, $X=\{x_1,x_2,\cdots,x_n\}$ and $Y=\{y_1,y_2,\cdots,y_m\}$, that follow different distributions. The MMD calculation formula between X and Y is as follows:

$$MMD(X,Y)=\left\|\frac{1}{n}\sum_{i=1}^{n}\varphi(x_i)-\frac{1}{m}\sum_{j=1}^{m}\varphi(y_j)\right\|_H^2 \quad (3)$$

In the Eq.3, $\|\bullet\|_H$ is RKHS; $\varphi(\bullet)$ is the function used to map the original variables to the RKHS.

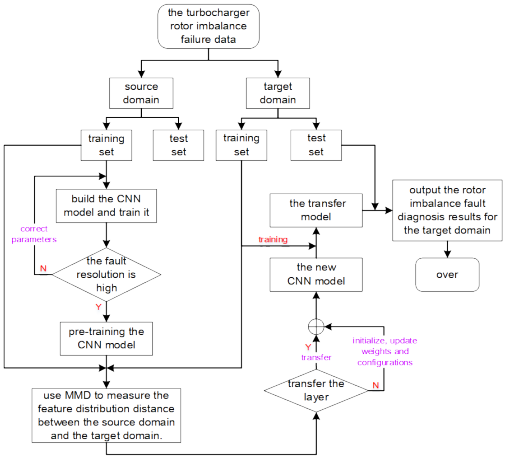

Figure 9. Fault diagnosis process of compressor rotor imbalance based on CNN transfer learning

4.2 Selection of simulation fault dataset for rotor imbalance

The classification results do not meet the expected performance when the time-domain simulation signals of the turbocharger are directly used to train the CNN model. Therefore, considering the physical significance of the time-domain and frequency-domain feature parameters at eight measurement points on the base of the turbocharger under six different speeds and three fault levels, as well as their variations with speed and fault conditions, the features most sensitive to fault classification and containing the highest information content are selected. At the same time, the performance of the features at different measurement points is evaluated. By comparing the signal quality and feature stability, the points with the most representative information are selected.

To overcome non-stationarity, capture local variations, and improve generalization, the simulated time-domain data are segmented into fifty segments of five seconds each. The final selected fault-sensitive features are mean amplitude, RMS value, and standard deviation, from measurement points 2, 4, and 6. Figure 10 shows that these are more sensitive to fault changes at point 6. Finally, the data set is split as shown in Table 2.

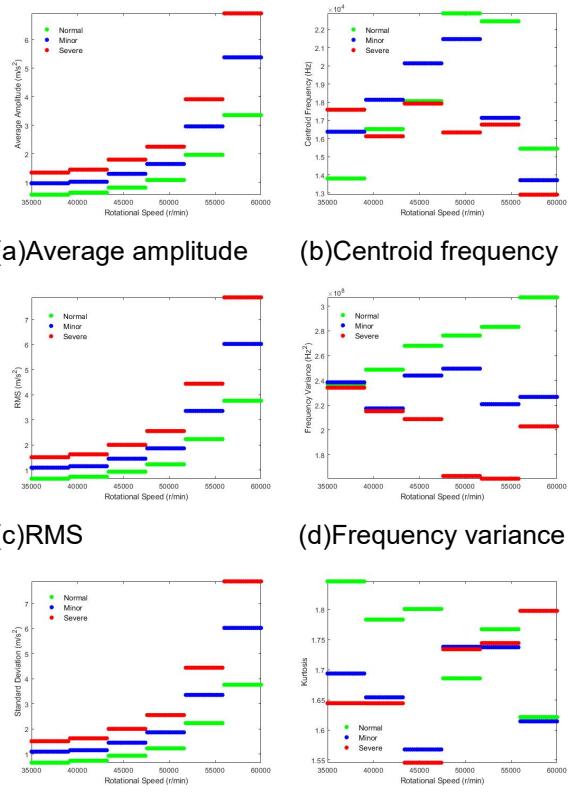

(a)Average amplitude (b)Centroid frequency

(c)RMS (d)Frequency variance

(e)Standard deviation (f)Kurtosis

Figure 10. Variation of feature parameters at measurement point 6 with speed and fault conditions

Dataset A is employed as the source domain, with datasets B, C, D, E, and F serving as the target domains. Each dataset comprises one hundred and fifty feature data points. The data is labeled according to the rotor imbalance fault types: the normal operating condition is labeled as 1, minor fault as 2, and severe fault as 3. The source and target domains are divided into test and training sets, with the results presented in Table 3.

Table 2. Composition of the dataset

Data set	Speed (r/min)	Degree of rotor imbalance fault	Characteristic samples
		Normal	50
A	60000	Minor	50
		Severe	50
		Normal	50
B	55000	Minor	50
		Severe	50
		Normal	50
C	50000	Minor	50
		Severe	50
		Normal	50
D	45000	Minor	50
		Severe	50
		Normal	50
E	40000	Minor	50
		Severe	50
		Normal	50
F	35000	Minor	50
		Severe	50

Table 3. Dataset split

Source domain A		Target domain B/C/D/E/F		Tab
Normal condition		Normal condition		1
10	40	40	10	
Minor faults		Minor faults		2
10	40	40	10	
Severe faults		Severe faults		3
10	40	40	10	
Test Set	Training Set	Test Set	Training Set	---
30	120	120	30	

4.3 Diagnostic performance analysis

4.3.1 Pre-training of the 1D-CNN model

The source domain dataset A is employed for the pre-training of the 1D-CNN model that has been constructed. To minimize the impact of randomness in the training results, each training session is conducted twenty times, and the average of the results is taken. The model exhibits an average accuracy of 100% for the diagnosis of rotor unbalanced faults, as illustrated in Figure 11.

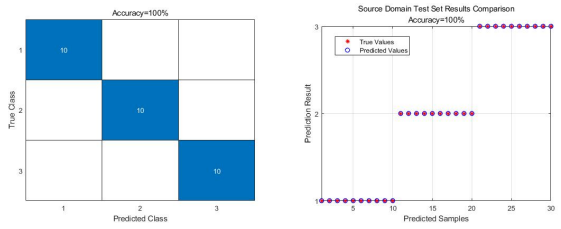

Figure 11. Fault diagnosis results of the CNN model in the source domain

4.3.2 Fault diagnosis based on the transfer model

Retaining the network structure and weight parameters of the fully trained CNN model. The maximum mean difference between the source and target domains on each convolutional and fully connected layer is calculated. A migration model is constructed and trained using the target domain data. Finally, the features extracted from the last layer of the migration model are mapped to a two-dimensional feature vector using the T-SNE algorithm. The transfer model, which is established based on the rotor imbalance fault dataset A at 60,000 rpm, is subsequently applied to the rotor imbalance fault diagnosis results of the other datasets B, C, D, E, and F at different speeds. The results of the fault diagnosis and the results of the reduction in the dimensionality of the features are presented in Figure 12 and Figure 13.

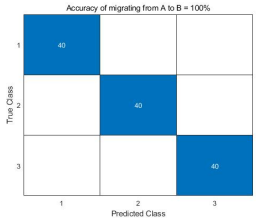

(a)Dataset B

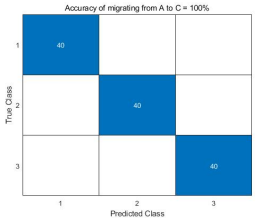

(b)Dataset C

(c)Dataset D

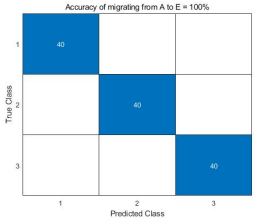

(d)Dataset E

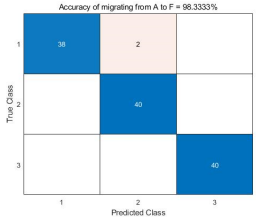

(e)Dataset F

Figure 12. Fault diagnosis results of the transfer model based on rotor imbalance fault dataset A

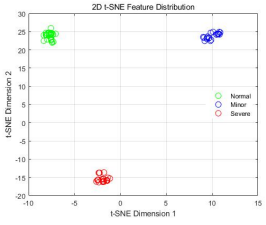

(a)Dataset B

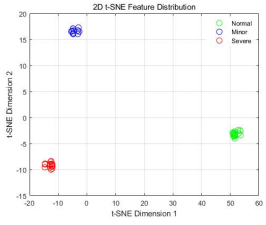

(b)Dataset C

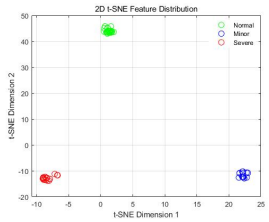

(a)Dataset D

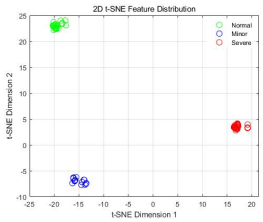

(b)Dataset E

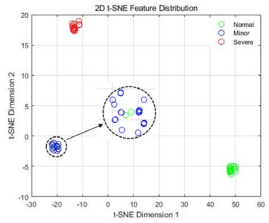

(e)Dataset F

Figure 13. Feature visualization of the transfer model based on rotor imbalance fault dataset A

Figure 12 and Figure 13 show that the transfer model has 100% fault diagnosis accuracy for rotor imbalance at 55,000 to 40,000 rpm. The characteristics of varying fault severities are discernible. For dataset F at 35,000 rpm, the fault diagnosis accuracy is 98.33% and some normal operating condition features are misclassified as mild faults. Overall, the transfer model presented in this paper exhibits notable adaptability in addressing rotor imbalance fault diagnosis for turbochargers across diverse operational speeds and fault severities. The model demonstrates a high degree of accuracy in fault diagnosis, with an average accuracy of 99.67%.

5 CONCLUSIONS

(1) The transient vibration response simulation model of the marine turbocharger is constructed. The characteristic parameters of the time-domain and frequency-domain vibration signals between the simulation and measurement of the turbocharger substructure under normal working conditions is compared and analyzed, and the errors of the comparison are no more than 5%, which demonstrate that the turbocharger vibration response simulation model is highly accurate and can be used to simulate and predict rotor failure.

(2) With the turbocharger speed increasing and the rotor imbalance exacerbated, the peak-to-peak value, root mean square value, and fundamental frequency peak value of the vibration acceleration at the base of the turbocharger all rise significantly, with the rate of increase continually growing. The patterns provide a basis for the selection of characteristics for fault diagnosis under variable operating conditions of the rotor.

(3) The transfer learning model of 1DCNN, based on the maximum mean difference criterion, achieves an accuracy of no less than 98.33% for fault classification recognition. It indicates that the model has strong adaptability across different operating conditions. It can serve as a reference for research into fault diagnosis technology for turbochargers under variable operating conditions.

6 ACKNOWLEDGMENTS

This work is supported by the project of ‘Research and development of high flow and reliability turbocharger for marine low-speed engine’ and the experiment of the turbocharger test bench of Chongqing Jiangzeng Shipbuilding Heavy Industry Co.

7 REFERENCES AND BIBLIOGRAPHY

[1] Peter Stålberg. 2023. Main engine damage report from an insurer’s point of view, Swedish Club, Sweden.

[2] Longkai W ,Guangfu B ,Xuejun L , et al. 2016. Effects of Unbalance Location on Dynamic Characteristics of High-speed Gasoline Engine Turbocharger with Floating Ring Bearings.Chinese Journal of Mechanical Engineering, 29(02):271-280.

[3] AHOBAL N, PRASAD S. 2019. Study of Vibration Characteristics of Unbalanced Overhanging Rotor. IOP Conference Series: Materials Science and Engineering, 577(1): 012140.

[4] KNOTEK J,NOVOTNY P,MARSALEK O,et al. 2015. The Influence of Rotor Unbalance on Turbocharger Rotor Dynamics. Journal of Middle European Construction& Design of Cars, 3(3):8-13.

[5] BIN G F,WANG L K,LI X J,et al. 2017. A Turbocharger Rotor Imbalance Control Method Based on Dynamic Characteristics: CN104458128B.

[6] SOUZA R M, NASCIMENTO E G S, MIRANDA U A, et al. 2021. Deep learning for diagnosis and classification of faults in industrial rotating machinery. Computers & Industrial Engineering, 153: 107060.

[7] JIAO J, ZHAO M, LIN J, et al. 2020. A comprehensive review on convolutional neural network in machine fault diagnosis. Neurocomputing, 417: 36-63.

[8] ZHANG T, DAI J. 2021. Mechanical fault diagnosis methods based on convolutional neural

network: a review. Journal of Physics: Conference Series, 1750(1): 012048.

[9] INCE T. 2019. Real-time broken rotor bar fault detection and classification by shallow 1D convolutional neural networks. Electrical Engineering, 101(2): 599-608.

[10] LEE K, HAN S, PHAM V H, et al. 2021. Multi-objective instance weighting-based deep transfer learning network for intelligent fault diagnosis. Applied Sciences, 11(5): 2370.

[11] KIM J, LEE J. 2022. Instance-based transfer learning method via modified domain-adversarial neural network with influence function: Applications to design metamodeling and fault diagnosis. Applied Soft Computing, 123: 108922.

[12] JAMIL F, VERSTRAETEN T, NOWÉ A, et al. 2022. A deep boosted transfer learning method for wind turbine gearbox fault detection. Renewable Energy, 197: 331-341.